Performance Analysis of Hybrid PPM-BPSK-SIM, PPM and BPSK-SIM Modulated FSO Link in a Controlled Fog Atmospheric Condition

A. Gatri[1], Z. Ghassemlooy[1], A. Valenzuela[2], and M. Mansourabadi[1]
[1]Optical Communications Research Group, NCRLab, Faculty of Engineering and Environment, Northumbria University, Newcastle Upon Tyne, UK
[2]Networks and data security, Bonn-Rhein-Sieg University of Applied Sciences, Sankt Augustin, Germany

***Abstract* — We report the performance of a free space optical (FSO) communications link employing binary phase shift keying subcarrier intensity modulation (BPSK-SIM), 4-ary pulse position modulation (4-PPM) and hybrid 4-PPM-BPSK-SIM, schemes in a controlled laboratory fog induced environment. Fog is generated and controlled along a dedicated indoor atmospheric chamber of length 6 m. We show the advantage of employing the 4-PPM-BPSK-SIM for FSO link over the BPSK-SIM and 4-PPM.**

Keywords* — *Free space optics, Hybrid PPM-BPSK-SIM BPSK-SIM, PPM, Fog, Visibility.

I. INTRODUCTION

Free space optical (FSO) communications [1] uses intensity modulated visible and infrared (IR) light spectrum for transmission of high-speed data over the free-space channel (both indoor and outdoor). FSO is seen as a complementary technology to the radio frequency (RF) and is a cost-effective alternative than renting expensive leased lines or digging and laying fiber between locations in applications including enterprise connectivity, mobile networks, "last-mile" access network, and satellite communications [2, 3, 20]. The FSO possibly is the only viable transmission technology for applications such as disaster recovery, defence, healthcare and sporting events where there is a need for rapid link set-up to provide fast, secure connectivity for audio, video and data transmission [4]. Despite its advantages, the FSO link performance is subject to impairment by atmospheric conditions, such as rain, temperature fluctuation and fog. There have been several studies on the impact of these effects on FSO links as reported in the literature [5-7, 10, 21].

Fog, compared to other atmospheric conditions, is the predominant source of attenuation. The fog attenuation ranges as high as 130 dB/km and 480 dB/km for a moderate continental and a dense maritime fog, respectively [8, 9, 22]. This reduces the FSO link availability from a few kilometers to hundreds of meters.

In the real world environment, it is very challenging to measure the effect of atmospheric fog under diverse circumstances, which was not done in this research. This is due to various reasons such as (i) a low probability of recurrence of dense fog events for visibility $V < 0.5$ km, and (ii) the difficulty in controlling and characteriszing aerosols in the atmosphere due to the inhomogeneous presence of aerosols along the FSO link path. Hence, an indoor atmospheric laboratory chamber is designed so that the measurement environment can be precisely controlled and measured; similar to the previous attempt [11].

The performance of the FSO link can be improved by employing an appropriate modulation scheme i.e. by appropriately trading-off between the power and bandwidth efficiencies [6, 27]. Among a number of modulation schemes studied for FSO channel, pulse position modulation (PPM) and binary phase shift keying subcarrier intensity modulation (BPSK-SIM) offer improved performance in the turbulence atmospheric environment [24-26]. In [28], a hybrid PPM-BPSK-SIM scheme based on PPM and BPSK-SIM was introduced and investigated in turbulence atmospheric environment. By combining the advantages of both the PPM which has high power efficiency and BPSK-SIM which has low sensitivity to the irradiance fluctuation as well as requiring no adaptive thresholding scheme compared to the widely used on-off keying scheme, it was proven that hybrid PPM-BPSK-SIM offers superior performance over PPM and BPSK for strong turbulence atmosphere. However, to the best of authors' knowledge, no experimental work is reported for the performance of PPM-BPSK-SIM in the presence of fog. Thus, we aim to study hybrid PPM-BPSK-SIM performances over dense fog conditions.

The paper is organized as follows: the characterization of the fog attenuation in a laboratory chamber and the hybrid modulation scheme are outlined in Section II, whereas the experimental and simulation set-up is introduced and explained in Section III. In Section IV, the results are discussed. The conclusions and future works are summarized in Section V.

II. THE CHARACTERIZATION OF THE FOG ATTENUATION IN A LABORATORY CHAMBER

A. Fog and Visibility

In practice, the meteorological visibility V is used to characterize fog attenuation in FSO systems. Applying Koschmieder´s law, V (km) can be calculated from the atmospheric attenuation coefficient β_λ and the visual threshold T_{th} at a wavelength of 550 nm, which is given as [12, 13]:

$$V = -\frac{10\log_{10}(T_{th})}{\beta_\lambda} \ , \tag{1}$$

where T_{th} is expressed in (dB/km).

In general, due to the physical properties of fog, such as particle size and the non-availability of particle dispersion, the fog induced attenuation of the optical signal is predicted using empirical models [18]. These models use the visibility data in order to estimate the fog induced attenuation. The empirical relationship, Kruse derived is given by [18]:

$$V(\text{km}) = \frac{10\log_{10}(T_{th})}{\beta_\lambda}\left(\frac{\lambda}{\lambda_0}\right)^{-q} \ , \tag{2}$$

where T_{th} is usually taken as 2%, λ_0 is equal to 550 nm and is the maximum sensitive wavelength for the human eye and *q* is the coefficient related to the particle size distribution in the atmosphere. Kruse´s model estimates the haze attenuation from visible to near infrared wavelengths. Kim modified Kruse`s model by applying predicted suppositions for the fog by re-defining the *q* values as follows [17]:

$$q = \begin{cases} 1.6 & \text{for } V > 50\,\text{km} \\ 1.3 & \text{for } 6 < V < 50\,\text{km} \\ 0.16V + 0.34 & \text{for } 1 < V < 6\,\text{km} \\ V - 0.5 & \text{for } 0.5 < V < 1\,\text{km} \\ 0 & \text{for } V < 0.5\,\text{km} \end{cases} . \tag{3}$$

Kim's model is more widely used and is closely matched with the measurement values and hence this model is adopted in this study.

B. FSO Link Performance with Fog

Measurements carried out in [11] showed the presence of fog when the relative humidity *H* of the real outdoor atmosphere (ROA) approaches 80%. The density of the resulting fog reaches 0.5 mg/cm^3 for *H* > 95%. Thus, under high water vapour concentration conditions, the water condenses into tiny water droplets of radius 1–20 µm in the atmosphere. There are different types of real outdoor fog (ROF), which are categorized on the basis of their formation mechanisms, such as convection fog, advection fog, precipitation fog, valley fog and steam fog [14]. The steam fog is localized and is created by the cold air passing over much warmer water or a moist land [14-16]. It is possible to simulate this form of fog in the laboratory by achieving *H* close to 95%. Hence, to mimic ROF, artificial fog can be generated by means of water-based steam.

Assuming $I(f)$ and $I(0)$ are the intensities of the received optical signals with and without fog, the transmittance *T* is given by Beer-Lambert`s law as [16]:

$$T = \frac{I(f)}{I(0)} = \exp(-\beta_\lambda z) \ , \tag{4}$$

where *z* is the propagation length.

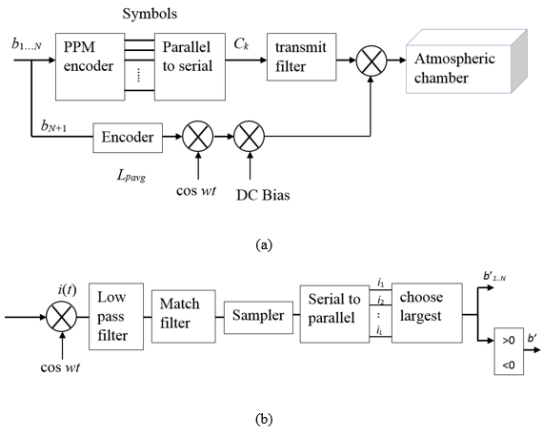

Fig. 1: Block diagram of L-PPM-BPSK-SIM FSO communication system: (a) transmitter and (b) receiver.

The link performance of a communication system can also be characterized by s the *Q*-factor, which is defined as [16]:

$$Q = T_0 \frac{|I_1 - I_0|}{\sigma_1 + \sigma_0} \ , \tag{5}$$

where T_0 denotes the maximum transmittance, I_1 and I_0 are the average detected signal currents for bit '1' and '0' respectively, whereas σ_1 and σ_0 are the standard deviation of the noise values for bit '1' and '0' respectively. With fog, and assuming that the ambient noise level does not change with fog density the *Q*-factor can be estimated as follows:

$$Q_{fog} = T_{fog} Q \, , \tag{6}$$

where T_{fog} is the transmittance measured in the presence of fog.

C. Hybrid PPM-BPSK- SIM

PPM-BPSK-SIM is a combination of PPM and BPSK-SIM schemes. As presented in the Figure 1, the transmitter comprises an *M*-bit PPM encoder, a parallel to serial converter, and a transmitter filter of a rectangular pulse shape of duration T_s defined as:

$$g(t) = \begin{cases} 1 & 0 \le t \le T_S \\ 0 & \text{else} \end{cases} . \tag{7}$$

For BPSK and PPM-BPSK, the standard RF demodulator is utilized to recover the transmitted symbol. The recovered sequence is then compared with the

transmitted sequence symbol-by-symbol to measure the slot (bit) error probability.

The resulting PPM symbols are then BPSK modulated with a radio frequency (RF) subcarrier. A DC bias is thereby added to the BPSK signal before the intensity modulation of the light source. The photocurrent at the output of the photodetector for one symbol stream is obtained by [28]:

$$i(t) = R\sum_{k=1}^{L} I_k(1+\zeta\cos(wt + x_k\pi)g(t-(k-1)T_s))) + A(t)\ , \quad (8)$$

where R is the photodetector responsivity, x_k is the codeword of PPM and the impulse response of the match filter $g(-t)$ is matched to the transmitter filter, I_k is the intensity of the received signal, ζ is the optional modulation index value and $A(t)$ is the additive white Gaussian noise (AWGN) with $\sigma^2 = N_0R_b/2$ and a zero mean value.

The received signal is passed through an electrical band-pass filter (BPF) within a minimum bandwidth of $2R_b$ centred at the RF sub-carrier frequency. Afterwards, the output signal from the BPF is down converted via the reference carrier signal cos (wt). Following the low pass filter, the matched filter and a sampler, demodulation is carried out by detecting the index of the slot within the largest amplitude in a symbol.

III. EXPERIMENTAL SETUP

The set-up used to assess the performance of proposed systems is shown in Figs. 1(a) and (b). It consists of an enclosed atmospheric chamber with a dimension of 600×30×30 cm^3, see Fig. 1(a). The chamber has two compartments, each with a vent to allow air circulation using a fan.

TABLE I.
PARAMETERS OF FSO COMMUNICATIONS LINK DEMONSTRATION

Parameter		**Value**
Data source	PRBS length	$2^{13}-1$
	Modulation	BPSK-SIM, 4-PPM , 4-PPM-BPSK
	Data rate	25 Mbps
Laser diode	Peak wavelength	830 nm
	Maximum optical power	10 mW
	Maximum peak to peak Voltage	500 mv
	Class	IIIb
	Beam size at aperture	5 mm × 2 mm
	Beam divergence	<10 mrad
	Modulation bandwidth	50 MHz
Photodetector (PDA36A)	Spectral range of Sensitivity	750– 1100 nm
	Active area	1 mm^2
	Half angle field of view	± 75 Deg
	Spectral sensitivity	0.60 A/W at 830 nm
	Rise and fall time	5 ns
	Reversed bias voltage	40 V
	Receiver sensitivity	- 32 dBm (at 25Mbps & BER = 10-6)
Optics	Lens type	Convex
	Focal length	20 cm
	Aperture	
Trans impedance amplifier (AD8015)		
	Bandwidth	240 MHz
	Gain	15 kΩ

The receiver front-end consists of an optical concentration lens and a PIN photodetector (PD) integrated with a wide-bandwidth transimpedance amplifier (TIA). The photocurrent of PD is amplified using the TIA output which is captured using a digital oscilloscope for further processing offline as presented in Fig. 1 (a).

The fog was generated using a fog machine (water steam) with 100% humidity to replicate the ROF. The fog is injected to the chamber at a rate of 0.97 m^3/sec. The fog intensity within the chamber is controlled by a number of fans and ventilation inlet/outlets allowing to manage the fog flux among the chamber homogeneously and control the visual contrast (transmittance) of the FSO link.

In order to ensure a fair comparison between the modulation schemes, the same average optical transmit power P_{tx} is maintained while the Q-factor and BER of the received signal are simultaneously measured for different fog conditions i.e. from low to high visibilities.

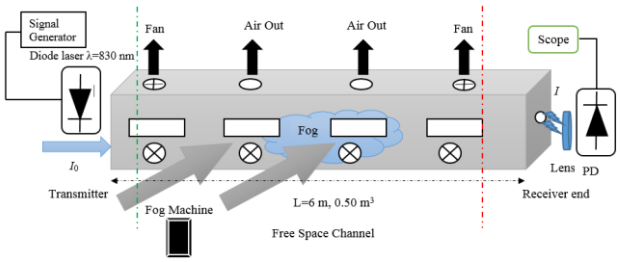

(a)

(b)

(c)

Fig. 2: (a) The block diagram of fog chamber and FSO link setup in the laboratory (b) the laboratory controlled atmospheric chamber and FSO link setup and Receiver end of the setup (c) Receiver end of the setup

IV. Results And Discussions

The experiment is carried out by filling the chamber with a controllable amount of fog to reach a range of very low to high visibility. In the experiment, fog is permitted to settle down homogenously in the chamber before the measurement is taken. The most important impact of the fog is the attenuation of the optical beam by Mie scattering and absorption. Both phenomena are caused by interaction of the particles with the electromagnetic waves spreading over the channel. This interaction depends on the characteristic size of obstacle or particle, refractive index and the wavelength of the optical beam.

Due to the very small refractive index value of the imaginary part, the absorption (Rayleigh scattering) in the IR waveband by fog and aerosols is negligible [14, 19].

The major contribution to the dispersion of the beam are particle sizes, which are close to the optical beam wavelength. Normally, both fog and haze are major contributors to the Mie scattering due to the optical wavelengths being in the order of 1000 - 1500 nm. As per the random nature and occurrence of the fog, its impact on the FSO link performance can promptly be measured and characterized by the visibility data [16, 17].

TABLE II.
MEASURED *T* AND VISIBILITY VALUES

Fog	**Dense**	**Thick**	**Moderate**	**Light**
T	< 0.31	0.31-0.71	0.71-0.8	0.8-0.9
V (m)	< 70	70-250	250-500	500-1000

Here, we evaluate the scattering coefficient β_λ using (4) corresponding to the measured *T* at 570 nm. The visibility *V* is evaluated using (3) with the wavelength independent model known as the Kim`s model for ranges < 500 m for different transmittance values, see Table II.

The *Q*-factor results depicted in Fig. 2 shows that Hybrid 4-PPM-BPSK-SIM and 4-PPM modulation signaling format are more robust to fog impairments on the FSO link than BPSK-SIM. The behaviour of the three modulations schemes under fog conditions are similar, however, in absolute terms at $T = 1$ the *Q*-factor is 8.5 for Hybrid 4-PPM-BPSK and 6.4 for 4-PPM and 4.3 for BPSK-SIM. On the other hand, Hybrid 4-PPM-BPSK and 4-PPM schemes overcome that values for $T > 0.2$. Fig. 2 illustrates the predominant gain of Hybrid 4-PPM-BPSK-SIM format over the rest of modulation schemes in moderate, Thick and dense fog conditions.

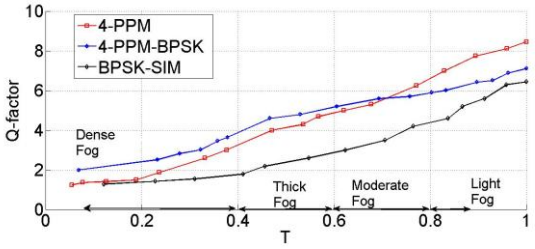

Fig. 3: Measured *Q*-factor values for Hybrid 4-PPM-BPSK, 4-PPM and BPSK-SIM received signals at same P_{tx} and 5Mbit/s data rate for different *T* link values and fog conditions.

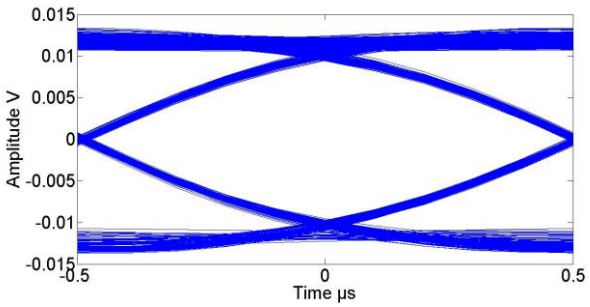

(b)

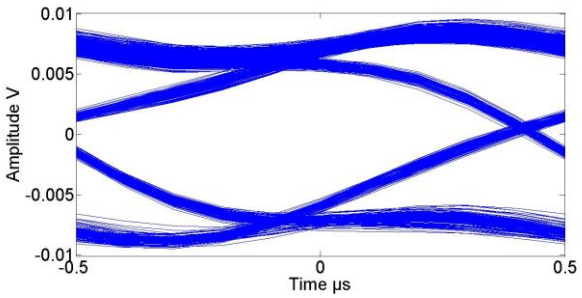

(b)

Fig. 4: The measured eye diagrams of the received Hybrid 4-PPM-BPSK-SIM signal at a data rate of 25 Mb/s with (a) no fog with *V*= 320 m, (b) fog attenuation with *V*= 100 m.

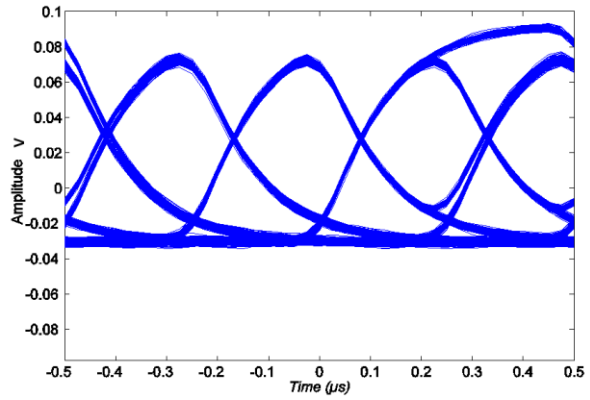

(a)

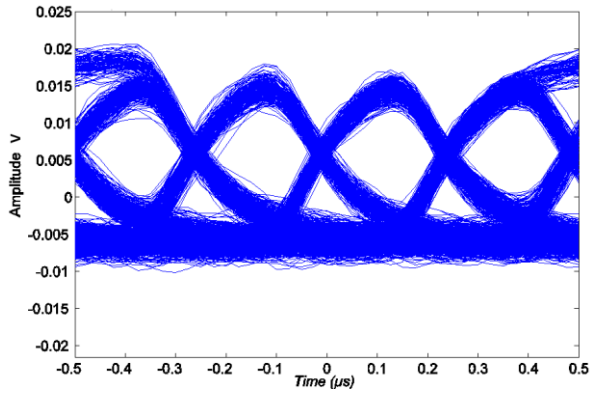

(b)

Fig. 5: The measured eye diagrams of the received 4-PPM signal at a data rate of 25 Mb/s with: (a) no fog with *V*= 320 m, (b) fog attenuation with *V*= 100 m.

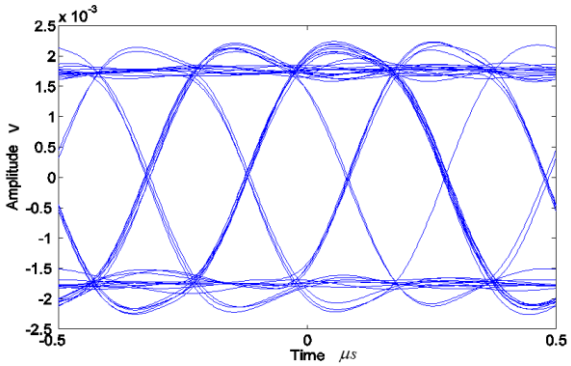

(a)

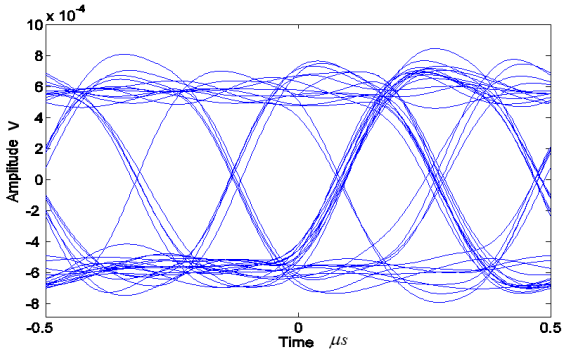

(b)

Fig. 6: The measured eye diagrams of the received SIM-BPSK signal with: (a) no fog condition with *V*= 320 m, data rate of 25 Mb/s, (b) Fog attenuation with *V*= 100 m.

The eye-opening is bigger for Hybrid 4-PPM-BPSK-SIM compared to 4-PPM and BPSK-SIM in the presence of fog attenuation, on the other hand, the eye-opening is bigger for 4-PPM than BPSK-SIM, indicating that Hybrid 4-PPM-BPSK is less sensitive to the intensity fluctuation under fog condition. Furthermore, Table III illustrates the visibility values corresponding to the measured values of *T*, the *Q*-factor corresponding to the BER P_{opt} of 0.60 dBm. As the amount of fog particles inside the chamber increases, the corresponding visibility decreases, thus resulting in increased scattering of the optical beam. This in turn causes the distribution of bits '1' and '0' to be more flat due to the loss in the height of the eye diagram.

TABLE III.
EXPERIMENTAL MEASURED VALUES FOR 0.60 DBM TRANSMITTED SIGNAL BER.

Visibility (m)	**BER Hybrid 4-PPM-BPSK-SIM**	**BER 4-PPM**	**BER BPSK-SIM**
450	9.479×10^{-17}	4.016×10^{-10}	9.86×10^{-9}
320	4.016×10^{-10}	1.898×10^{-7}	3.33×10^{-7}
140	2×10^{-3}	13.4×10^{-3}	25×10^{-3}
100	10.7×10^{-4}	81.9×10^{-3}	22.7×10^{-2}
65	62×10^{-3}	66.8×10^{-2}	136×10^{-2}

V. CONCLUSION

The experimental evaluation of the performance of Hybrid 4-PPM-BPSK-SIM, 4-PPM and BPSK-SIM modulation schemes was carried out under the effect of fog in a controlled laboratory test-bed and the proposed hybrid modulation is compared with 4-PPM and BPSK-SIM. The effects of low to high visibility on the FSO link BER performance in the presence of fog was measured and investigated. Obtained results indicate the dependency of the fog intensity variation on the

performance of the FSO link. Furthermore, the hybrid 4-PPM-BPSK-SIM signalling format offers improved resistance to the thick fog impairment than the 4-PPM and BPSK-SIM. The BER characteristics of the three modulations over fog induced channel are studied. The results show that the use of hybrid 4-PPM-BPSK-SIM improves the performance of the FSO system performance over thick fog channel. More work to investigate different positions among the FSO links and more severe fog attenuation over the FSO links and applying more optic components over the chamber is going on and will be published in due course.

AKNOLEDGMENT

This work is supported by the EU COST Action IC1101.

REFERENCES

[1] R.Nebuloni, C. Capsoni, "Effects of Adverse Weather on Free Space Optics",*In book: Optical Wireless Communications*, pp.47-68, January 2016.

[2] M. Uysal et al, "Optical Wireless Communications An Emerging Technology". *Signals and Communication Technology*, pp. 1-23, September 2016.

[3] Cheikh A. B. Dath, Modou Mbaye, Ndeye Arame Boye Faye, Ahmadou Wague, "Reliability of FSO systems in Sahel region: a case study of the major city of Dakar", *International Journal of Engineering Science and Innovative Technology (IJESIT)*, Volume 4, Issue 1, pp. 368-370, January 2015.

[4] L. Joe *et al*., "Future Army Bandwidth Needs and Capabilities," Report for the U.S. Army by RAND Corporation, 2004.

[5] D. Kedar, and S. Arnon, "Optical wireless communication through fog in the presence of pointing errors," *Appl. Opt*. 42, 4946-4954, 2003.

[6] In K.Son, S.Maoa, "A Survey of Free Space Optical Networks",*Digital Communications and Networks, in Science direct,*pp. 1-15,November 2016.

[7] Z. Hajjarian, and M. Kavehrad, "Using MIMO transmissions in free space optical communications in presence of clouds and turbulence," *in Proc. SPIE* 7199, 1-12 (2009).

[8] K.W. Fischera, M.R. Witiwb, E. Eisenberg:" Optical attenuation in fog at a wavelength of 1.55 micrometers", *Third International Conference on Fog, Fog Collection and Dew, Atmospheric research*, vol. 87, pp. 252-258, 2008.

[9] M.N.O. Sadiku, S.M. Musa, "Free Space Optical Communications: An Overview," *European Scientific Journal*, vol.12(9), pp. 55-68, February 2016.

[10] Strickland, B. R., Lavan, M. J., Woodbridge, E., and Chan, V., Effects of fog on the bit -error rate of a free space laser communication system, *journal of applied optics*, vol.38, pp. 424-431, 1999.

[11] M. S. Awan, L. C. Horwath, S. S. Muhammad, E. Leitgeb, F. Nadeem, and M. S. Khan, "Characterization of fog and snow attenuations for free-space optical propagation," *Journal of Communications*, vol. 4, pp. 533-545, 2009.

[12] S. S. Muhammad, B. Flecker, E. Leitgeb, and M. Gebhart, "Characterization of fog attenuation in terrestrial free space links," *Journal of Optical Engineering*, vol. 46, pp. 066001-066006, 2007.

[13] Z. Ghassemlooy, H. Le Minh, S. Rajbhandari, J. Perez, and M. Ijaz, "Performance analysis of ethernet/fast-ethernet free space optical communications in a controlled weak turbulence condition," *J. Lightw. Technol*., vol. 30, pp. 2188–2194, 2012.

[14] S. V. Kartalopoulos, "Free space optical networks for ultrabroad band services," *J. Wiley & Sons*, New Jersey, pp. 35-36, 2011.

[15] J. Mikołajczyk, Z.Bielecki, M. Bugajski, J.Piotrowski, J. Wojtas, W.Gawron, and D. Szabra, A.Prokopiuk, "Analysis of Free-Space Optics Development," *Metrol. Meas. Syst.*, Vol. 24, pp.653–674, December 2017.

[16] M. Jonasz and G. Fournier, "Light scattering by particles in water: theoretical and experimental foundations," *Elsevier Inc*, Oxford, UK, 2007.

[17] I. Isaac. Kim, B. McArthur, and E. Korevaar, "Comparison of laser beam propagation at 785 nm and 1550 nm in fog and haze for optical wireless communications," *SPIE Proceedings*: Optical Wireless Communications III, vol. 4214, pp. 26-37, 2001.

[18] F. Nadeem, T. Javornik, E. Leitgeb, V. Kvicera,G. Kandus, „Continental Fog Attenuation Empirical Relationship from Measured Visibility Data", *in Journal of Radio Engineering*, vol. 19 Issue 4, pp. 596-600, Dec 2010,

[19] I. I. Kim, B. McArthur and E. Korevaar, "Comparison of laser beam propagation at 785 nm and 1550 nm in fog and haze for optical wireless communications," *in Proc. SPIE* 4214, Boston, MA, pp. 26-37, USA 2001.

[20] Z. Ghassemlooy, W. Popoola and S. Rajbhandari, "Optical Wireless Communications: System and Channel Modelling with MATLAB®", *CRC Press*, New York August 2012, pp. 111-115.

[21] Fadhil, H. A., Amphawan, A.H., Shamsuddin, A. B., Thanaa Hussein A.H Al-Khafaji, M. R., Aljunid, S. A., and Nasim Ahmed, "optimization of free space optics parameters: An optimum solution for bad weather conditions," *Elsevier, Optik*, vol.124, pp. 3969-3973, 2013.

[22] J.Tóth, L. Ovseník and J. Turán, "Advanced wireless communication systems Free space optics: Atmosphere monitoring proposal (Fog and Visibility)," *IEEE 13th International Scientific Conference on Informatics*, pp.281 - 285, 2015.

[23] Ijaz, M.; Ghassemlooy, Z.; Pesek, J.; et al, "Modeling of Fog and Smoke Attenuation in Free Space Optical Communications Link under Controlled Laboratory Conditions," *Journal of Lightwave Technology* Volume: 31, pp. 1720-1726.

[24] M.R. Alam, S. Faruque, "Comparison of different modulation techniques for free space laser communication", *2015 IEEE International Conference on Electro/Information Technology (EIT) on*, pp. 637 – 640, 2015.

[25] T. Ohtsuki, "Multiple-subcarrier modulation in optical wireless communications," *IEEE Communication Magazine*, vol. 41, pp. 74-79, March, 2003.

[26] Muhammad Ijaz, "Experimental Characterisation and Modelling of Atmospheric Fog and Turbulence in FSO", *in School of Computing, Engineering and Information Sciences, Doctor of Philosophy Newcastle*: University of Northumbria, 2013.

[27] H. Zhang; H. Li; X. Dongya; C.Chaom, "Performance Analysis of Different Modulation Techniques for Free-Space Optical Communication System", *in Telkomnika*, Vol. 13 Issue 3, pp. 880-888, 2015.

[28] M. Faridzadeh; A. Gholami; Z. Ghassemlooy; S. Rajbhandari, "Hybrid PPM-BPSK subcarrier intensity modulation for free space optical communications," *Journal of the Optical Society of America. A, Optics, Image Science, and Vision*, Volume 29 (8), pp. 1680-1685. Aug 2012.